X-ray-absorption near-edge structure study in mixed-valent samarium systems

E. Beaurepaire and J. P. Kappler
IPCMS-GEMME 4 rue Blaise pascal, 67070 Strasbourg CEDEX, France

G. Krill
Laboratoire de Physique des Solides, Universite de Nancy I, Boîte Postale 239, 54506 Vandoeuvre les Nancy, France
(Received 14 September 1989)

We report measurements of x-ray-absorption near-edge structures (XANES) 20–100 eV above the L_{III} edge of Sm in mixed-valence SmS- and SmB_6-based systems. We show that the XANES measurements are strongly dependent on temperature, hydrostatic pressure, and sample composition. A phenomenological model is developed to interpret the data, indicating the sensitivity of the spectra to any modification of the Sm valence, interatomic distances, or atomic relaxation. Atomic relaxation effects could be determined for a large number of compounds. We discuss the static or dynamic nature of the valence mixing from the importance of atomic relaxation effects deduced from our data. Possible complications arising from final-state effects and their influence on our interpretations are addressed.

I. INTRODUCTION

The electronic structure of rare-earth (RE) systems is characterized by $4f$ shells nearly localized and interacting with other orbitals via a hybridization parameter V_{kf} much smaller than the intrasite Coulomb correlation energy U_{ff} and conduction bandwidth W. For Ce-, Sm-, Eu-, Tm-, and Yb-based systems, whose $4f$ levels lie close to the Fermi level, hybridization effects may lead to heavy-fermion or to mixed-valence behavior. The theoretical treatment of such phenomena is a true many-body problem that is often described by the one-impurity Anderson model.[1] A breakthrough in its solution has been obtained only recently, when it was realized that both excited and ground states can be obtained by an expansion over $1/N_f$ (N_f is the degeneracy of the $4f$ configuration).[2] This approach has been widely used in order to study, from a microscopic point of view, the nature of the ground state and the spectroscopic properties of Ce systems. One important conclusion of such studies is that, because of the large hybridization V_{kf}, the $4f$ occupancy has a lower limit near 0.7 in Ce intermetallics[3] and 0.5 in formally tetravalent insulators;[4] some recent works on Yb systems pointed out the occurrence of similar hybridization effects.[5]

Since the hybridization and phonon energy scales are comparable, anomalies can occur in bulk moduli and phonon dispersion curves due to the electron-phonon interaction. Such anomalies are indeed observed in some systems like TmSe (Ref. 6) or $Sm_{0.79}Y_{0.29}S$,[7] but not in others (e.g., $CePd_3$ or $CeSn_3$).[8,9]

An intuitive unifying picture was proposed recently,[10] assuming that high-frequency phonon modes (as compared to the charge fluctuation rate) probe a static mixture of say $4f^n$ and $4f^{n+1}$ ions, and therefore the corresponding phonon frequency is intermediate between the expected values for fictitious integer valent systems. On the other hand, a phonon softening is expected in peculiar crystallographic directions in the situation where the phonon frequency is lower than the charge fluctuation rate. It is shown in Ref. 10 that the nature of the phonon anomalies is in agreement with the estimated charge fluctuation rates for a large number of mixed-valent compounds.

Clearly, in order to further research this problem and to bear out theoretical models, it is convenient to give experimental evidence of shell breathing modes associated with $4f$ charge fluctuations. Such shell breathing can give rise to atomic relaxation effects because of the $\simeq 0.15$ Å difference in size between $4f^n$ and $4f^{n+1}$ ions. Extended x-ray-absorption fine structures (EXAFS) above the RE L_{III} edge is a local probe that seems to be well studied to the study of such atomic relaxations. EXAFS results have been obtained on mixed valence SmS alloys and TmSe, and it has been concluded that no atomic relaxation occurs in such compounds (only a single RE–first-neighbor interatomic distance is evidenced).[11–13] However, such a conclusion remains confusing since it depends on the hypothesis made about the use of one[11a,12] or two[11b] threshold energies in EXAFS data analysis. This is in variance with the edge structure itself, where two thresholds are clearly identified in L_{III} absorption spectra of mixed-valent systems,[14] because of the two possible final-state channels $2p^6 4f^n \rightarrow 2p^5 4f^n 5\epsilon d$ and $2p^6 4f^{n+1} \rightarrow 2p^5 4f^{n+1} 5\epsilon d$, separated in energy by about 7 eV. Subsequent works on this field have shown that a definitive solution to the EXAFS problem cannot be obtained from a conventional analysis if quantitative information is required, due to correlations between the different parameters: energy thresholds, atomic relaxation, and Debye-Waller factors.[15] Nevertheless, accurate atomic relaxation values ($\Delta R < 0.05$ Å) can be proposed only in the few cases where a careful analysis of the amplitude and phase of

the EXAFS signal have been performed using two threshold energies.[16]

In order to overcome these difficulties, we have recently shown that a study of the x-ray-absorption near-edge structure (XANES) regime, intermediate between the EXAFS and threshold range can bring new information on this problem.[20] As will be demonstrated in this paper, the main advantage of XANES is its sensitivity to both edge splitting and interatomic distance effects. We have explained the data in a phenomenological model that indicates the importance of using two thresholds and atomic relaxations in mixed-valent systems. We were then able to show that homogeneous (dynamic) mixed-valent systems are characterized by weak atomic relaxation effects ($\Delta R < 0.1$ Å) in opposition to the case of inhomogeneous (site dependent) valence mixing, where $\Delta R > 0.1$ Å.

Another important motivation for performing a XANES analysis in mixed-valent RE systems is the lack of a general understanding of many-body effects in x-ray-absorption spectra from the edge up to the EXAFS regime; *a priori* the EXAFS description (regarding many-body effects) should be conceptually similar to the case of XPS (Ref. 4) (since the photoelectron kinetic energy range is the same), whose theoretical description is satisfactory. On the other hand, experimental[17,18] and theoretical works[19] on the L_{III} edge region of light RE systems have shown that the final state is more complex and involves the photoelectron itself. Moreover, the transition between these two extreme situations is still an open question.

The purpose of this paper, in connection with the above-mentioned problems, is to discuss the validity of our description[20] and the results obtained in systems where the RE valence presents strong variations on temperature, hydrostatic pressure, and substitution effects, namely (Sm,R)S with R =Y,Gd, Sm(S,A) with A =P,As, and (Sm,M)B_6 with M =Sr,Yb.

II. EXPERIMENTAL

Sample fabrication[21,22] and preparation for L_{III} absorption[23] are reported elsewhere. Best SmS samples (judged from the intensity of the Sm^{3+} structure) were obtained by spreading powder filtered to 20μm on Scotch tape (avoiding crushing). The absorption experiments have been obtained at the EXAFS II set up at the Laboratoire pour l'Utilisation du Rayonnement Electromagnétique (LURE) Orsay. Details can be found in Ref. 20 and references therein. The sample's temperature could be varied between 30 and 300 K using an He flow cryostat. The experiments have been performed cooling down the samples to the lowest temperature, and then gradually heating them up.

We have also analyzed the previously reported[24] XANES part of L_{III} experiments under high pressure on SmB_6. After a pre-edge background substraction the L_{III} data are normalized in the following way: for edge studies the spectra are normalized to 1 averaging the signal up to $\simeq$100 eV after the "white line"; for XANES studies the spectra are normalized at the threshold energy, after substraction of a smooth polynomial fit of the after edge region.

III. EDGE RESULTS

L_{III} edges corresponding to the SmS and SmB_6 series are represented in Fig. 1. Because of the high density of dipole allowed 5d states above the Fermi level in RE systems, a strong white line is observed at the edge.[25] Moreover, the thresholds associated with Sm^{2+} and Sm^{3+} ions are split by 7 eV due to the final-state interaction between the core hole and the 4f shell; this allows an observation of the mixed-valence ground state in various systems and a quantitative estimate of the valence to be made. These thresholds are observed in our experiments, respectively, around 6712 and 6719 eV. We shall briefly discuss here the physical properties of SmB_6 and SmS alloys, and comment on L_{III} results.

The SmS compound is well known to be a semiconductor, where Sm ions are in a divalent ($4f^6$) ground state. Several works have shown that the Sm valence can vary upon doping either on the cation [with, e.g., P (Ref. 26) and As (Ref. 27) atoms] or on the anion [(Ref. 28), Gd (Ref. 29), or other RE atoms] sublattice. Below a critical concentration ($x_c \simeq 0.05$ for P,As, $x_c \simeq 0.15$ for Y,Gd) the samples remain semiconducting, but the valence of Sm atoms around the impurities changes to 3 (this mechanism has been demonstrated at least in the case of O,P,As), leading to the so-called inhomogeneous mixed-valent (IMV) ground state. At higher concentration, samples are metallic (golden phase) and present the properties of homogeneous mixed-valent systems (HMV) with $2.5 \leq v \leq 3$. The $Sm_{1-x}Y_xS$ and $Sm_xGd_{1-x}S$ samples with $x \simeq 0.2$ present an interesting transition from the metallic phase at room temperature to the semiconducting one (below $\simeq$150 K). This transition is related to a large valence variation resulting in a modification of the L_{III} spectra, as shown in Fig. 1 (see also Ref. 11).

In order to obtain the parameters relevant for our XANES analysis (see next section) the L_{III} data have been fitted using a procedure described elsewhere.[30] We found, in agreement with Ref. 31, that a better simulation of the SmS spectrum is obtained using two white lines (full line in Fig. 1) rather than one (dashed line); this additional structure has a relative intensity of 8% leading to an L_{III} valence v =2.08 that is apparently conflicting with the physical properties of this system. The origin of this extra contribution has been recently addressed:[32] Theoretical and experimental reasons suggest that it is a multiple-scattering resonance since it is also present in both calculated and isostructural trivalent reference spectra (see, e.g., GdS in Fig. 1). The L_{III} valence of Sm corrected for this effect is reported in Table I for (Sm,R)S and Sm(S,A) with R =Y,Gd and A =P,As. These values are in qualitative agreement (± 0.1) with those obtained from other absorption experimental setup or analysis procedures.[33] We therefore confirm the rapid increase of the Sm valence in the inhomogeneous phase and

the jump around x_c at room temperature. The Sm valence is close to 2.6 just after the volume collapse [as it is in the case of the pressure induced transition of SmS (Ref. 31)] and converges towards 3 at higher concentrations. Interestingly, the behavior of $Sm_{0.75}R_{0.25}S$ at room temperature is intermediate between those of the semiconducting and metallic phases obtained by cation substitution, and at low temperature the valence is closer to the values of the black phase.

Similar results, reported in Fig. 1 for some $(Sm,M)B_6$ alloys, are in agreement with an earlier detailed study.[21] We found a Sm L_{III} valence of 2.63 in SmB_6. It has been observed[21] that a decrease of the average number of conduction electrons (e.g., by Sr^{2+} or Yb^{2+} substitution) leads to a larger Sm valence, whereas the opposite occurs if the number of conduction electrons increases (Y^{3+}, La^{3+}, or Th^{4+} substitution). This effect is independent of the size of the substitutional atoms. As a matter of fact, we found that the Sm valence nearly reachs 2.92 in $Sm_{0.12}Yb_{0.88}B_6$ but saturates to 2.35, e.g., in $Sm_{0.17}Yb_{0.83}B_6$.

IV. PRESENTATION AND DISCUSSION OF XANES RESULTS

A. Many-body versus one-electron description

As illustrated earlier, and in agreement with many other studies,[33] the mixed-valent ground state of RE atoms produces a characteristic splitting of the L_{III} edge. In a previous work,[34] we focused our attention on the first x-ray-absorption fine structure about 30 eV above the RE L_{III} threshold in several mixed-valent systems ($CePd_3$, $YbAl_2$, and SmB_6): We observed that the XANES in these compounds also presents a splitting between $4f^n$ and $4f^{n+1}$ contributions.[34] However, in order to provide a quantitative explanation of XANES in such compounds, one should be able to separate in the spectra the contributions arising from many-body and structural effects. It is not our purpose here to give a formal description of the x-ray-absorption process in its generality. We restrict our discussion to qualitative arguments that justify the approach we used in Ref. 20.

The x-ray-absorption coefficient in the electric dipolar

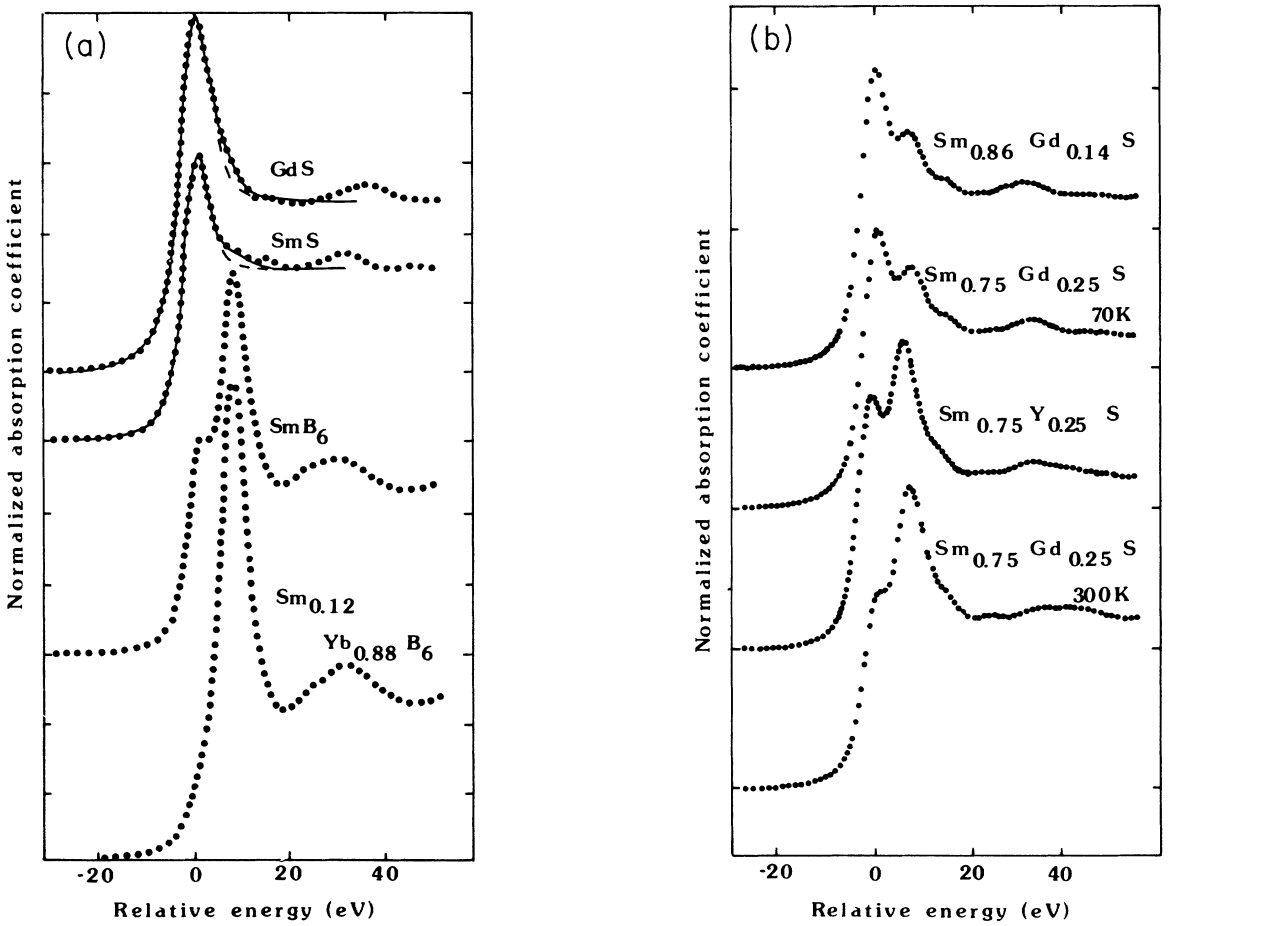

FIG. 1. L_{III} edge of (a) Gd in GdS and Sm in SmS and SmB_6 alloys, (b) Sm in SmS alloys. The energy origin is set at the maximum of Gd or Sm^{2+} white lines. Full lines (resp. dashed) in the spectra of SmS and GdS correspond to simulations using one (resp. two) white lines, as discussed in text. The spectra are recorded at 300 K when the temperature is not mentioned.

TABLE I. XANES parameters in SmS alloys and SmB_6. x in $Sm_{1-x}Y_xS$; y in $Sm_{1-y}Gd_yS$. n_f (reduced $4f$ count), ΔE (edge splitting), and ΔR (atomic relaxation) are defined in text. D_a (resp. D_1) is the average Sm first-neighbors interatomic distance deduced from the XANES analysis (resp. from x-ray diffraction). H (resp. I) means homogeneous (resp. inhomogeneous) mixed-valence compound.

Compound	n_f (L_{III})	n_f (XANES)	ΔE (eV)	ΔR (Å)	D_a (Å)	D_1 (Å)	
SmB_6 $P=0$	0.37	0.43	6.95	0.01	4.13	4.134	H
$P=100$ kbar	0.21	0.2	6.45	0	4.01	4.02[a]	H
$Sm_{0.35}Sr_{0.65}B_6$	0.21	0.2	6.9	0	4.18	4.17	H
$SmS_{0.9}P_{0.1}$	0.4	0.35	7.3	0	2.85	2.85	H
$x=0.25$ $T=300$ K	0.55	0.6	7.3	0.03	2.855	2.84[b]	H
$x=0.25$ $T=70$ K	0.71	0.78	7.45	0.04	2.89	2.88	H
$y=0.25$ $T=300$ K	0.45	0.42	7.5	0.025	2.84	2.84[c]	H
$y=0.25$ $T=40$ K	0.75	0.72	7.5	0.085	2.89		
$y=0.18$ $T=300$ K	0.49	0.45	7.5	0.05	2.85	2.84[c]	H
$y=0.18$ $T=70$ K	0.73	0.75	7.5	0.07	2.89	2.91	
$y=0.14$ $T=300$ K	0.81	0.84	7.55	0.13	2.93	2.935[c]	I

[a]From Ref. 52.
[b]From Ref. 27.
[c]From Ref. 29.

approximation is usually expressed by the Fermi golden rule

$$\mu(\hbar\omega) \propto \sum_f |\langle \psi_f | \varepsilon \cdot \mathbf{r} | \psi_i \rangle|^2 \delta(\hbar\omega + E_i - E_f) , \quad (1)$$

where i labels denote the ground state and f the final state (with a $2p$ core hole and an additional conduction electron above the Fermi energy).

In the one electron approximation, μ is replaced by μ_{oe} where the wave functions entering in (1) are obtained either from a band-structure calculation[25,35,36] or, in the real space, applying the multiple-scattering formalism.[37] This approximation is of course not valid for mixed-valent systems so that such a calculation cannot reproduce the double-edge structure for instance observed in α-Ce.[38]

However, the expansion of (1) to IMV systems is trivial, since one can distinguish the contribution of different sites, where Sm atoms have distinct valence states so that

$$\mu(\hbar\omega) = (1-n_f)\mu_n(\hbar\omega) + n_f\mu_{n+1}(\hbar\omega) , \quad (2)$$

here μ_{n+1} (μ_n) are the contributions to the spectra of Sm^{+2} (Sm^{3+}) atoms and n_f the reduced $4f$ count ($n_f=0$ for Sm^{3+} and 1 for Sm^{2+}). The energy shift between these two contributions is large due to the Coulomb attraction between the core hole and the $4f$ states ($U_{cf} \simeq 7$ eV).

The case of HMV systems is more difficult since ψ_f and ψ_i are a solution of many-body Hamiltonians. If the many-body processes do not include the photoelectron (in a first step we shall assume that it is a good approximation), μ can be expressed by a convolution[39]

$$\mu = \mu_{oe} S \quad (3)$$

μ_{oe} is defined above and S is the $2p$ core-level photoemission spectral function. S is expected to present in Sm mixed-valent systems two peaks (attributed to $4f^n$ and $4f^{n+1}$ configurations with a relative weight related to the valence), by analogy with the $3d$ XPS spectra.[40] Therefore, each structure in μ_{oe} appears split in μ (in agreement with the results of Ref. 34) so that the Eq. (2) follows for HMV systems too. The great advantage of this method is that now μ_n and μ_{n+1} can be estimated from suitable experimental references or from one-electron calculations for integral valent systems.

The theoretical tools mentioned before (multiple scattering or band-structure approach) can be used in order to achieve this goal. Indeed, the ability of the theory to reproduce L spectra of normal RE systems such as the metals[24] or SmS (Ref. 32) have been demonstrated, this suggests that a one-electron picture is valid in this case. However, in order to perform a simulation of experimental data starting from Eq. (2), it seems more suitable to use experimental reference spectra μ_n and μ_{n+1} corresponding to the same local surrounding (type of atoms, bond lengths, and angles) of the absorber atom as in the mixed-valent system under study. Since in the applications presented here we could obtain reference systems preserving the crystallographic structure, only variations of bond lengths should be taken into account.

We have based our analysis on experimental and theoretical works showing that, over a large energy range, the absorption coefficient scales as

$$(E-E_0)R^2 , \quad (4)$$

where E_0 is the threshold energy and R a relevant interatomic distance. This rule has been applied to various systems[35,41] including RE metals.[38] In fact such a scaling law can be derived from multiple-scattering formalism, identifying R with the multiple-scattering path length and E_0 with the interstitial potential in a muffin-tin approximation.[42] Therefore it is reasonable to estimate μ_n and μ_{n+1} in the relation (2) from an experimental reference spectrum rescaling the energy axis according to Eq. (4).

B. Phenomenological description of XANES spectra in MV systems

We illustrate here how XANES spectra in mixed-valent (MV) materials presented in Sec. III can be ana-

lyzed developing the ideas presented earlier, in order to get information on atomic relaxation effects. However, in the cases under study we cannot exhibit reference spectra for both $4f^n$ and $4f^{n+1}$ situations, thus we propose to build the missing reference from the existing one by (i) shifting the energy origin by $\pm\Delta E$ in agreement with the edge splitting; (ii) taking into account the variation of interatomic distances according to the scaling law (4). It has been shown[20] that this assumption leads to reasonable results for the description of XANES in amorphous Eu_xPd_{1-x} alloys, where Eu valence varies from 3 to 2 as x increases.

Since EXAFS studies underlined that the threshold splitting is an important parameter to determine, we first tested the influence of ΔE on the spectra for a fictitious SmS compound with $n_f=0.5$ using the relation

$$\mu(E)=n_f\mu_0(E)+(1-n_f)\mu_0(E-\Delta E)\ ,$$

where μ_0 is the measured absorption coefficient for SmS. In Fig. 2 the energy splitting between $4f^5$ and $4f^6$ configurations is allowed to vary from 0 to 9 eV (compare with the value obtained from the fits of the edge: $\Delta E\simeq 7.3$ eV). Though a clear splitting of the structures labeled B and C on the figure is not observed for the set of parameters we used, a clear dependance on ΔE appears both on the shape and intensity of these spectral features.

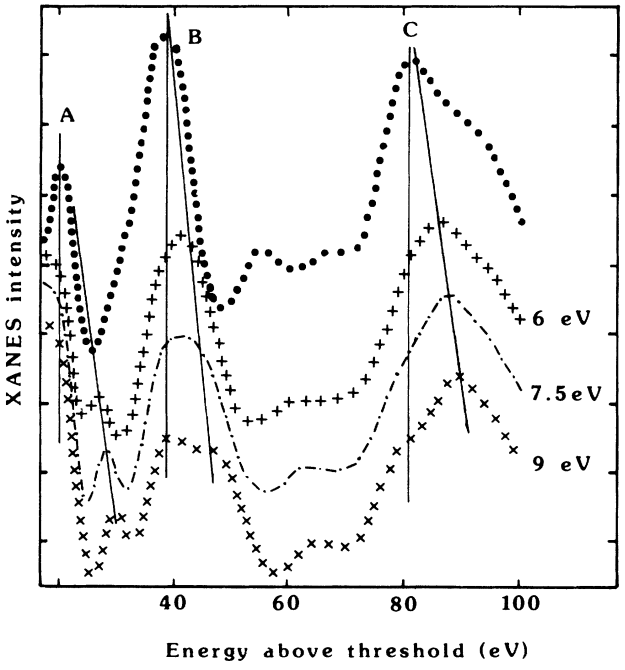

FIG. 2. Simulations (see text) of the L_{III} XANES of fictitious SmS compounds assuming the valence $v=2.5$, lattice constant $a=5.82$ Å, and different values of the energy splitting ΔE. A graduation of the vertical scale represents 2% of the edge jump. The energy zero is given by the onset of transitions $2p^64f^6\rightarrow 2p^54f^65d$ as deduced from the analysis of the "white line" (see text).

In presence of electron-phonon interaction and f-d hybridization, the energy of the MV ground state may present two minima (d_n and d_{n+1}) as a function of the interatomic distance.[43] It is therefore relevant to test the possibility of two interatomic distances associated with $4f^n$ and $4f^{n+1}$ even in HMV systems, thus defining the atomic relaxation as $\Delta R=d_n-d_{n+1}$. Such atomic relaxations are explicitly taken into account in the XANES simulations of Fig. 3, in the same way as previously but fixing $\Delta E=7.5$ eV. Because the $E\cdot d^2$ rule is now applied to the individual spectra corresponding to Sm^{2+} and Sm^{3+} with different interatomic distances when building the simulations, the splitting of energy between the structures such as $B(Sm^{2+})$ and $B(Sm^{3+})$ is increasing with ΔR (see Fig. 3). For the lowest values of ΔR, shoulders are first appearing in the fine structures recalling the results of Ref. 42. For $\Delta R=0.1$ Å, two series of structures corresponding to $4f^n$ and $4f^{n+1}$ are clearly resolved.

Figures 2 and 3 show the sensitivity of the simulations to the various input parameters so that quantitative informations on atomic relaxation can be obtained. Nevertheless, the values of ΔR and ΔE are slightly correlated, e.g., the simulations with ($\Delta E=9$ eV and $\Delta R=0$) and ($\Delta E=7.5$ eV and $\Delta R=0.04$ eV) can only be distinguished by superposition of the spectra. In fact, we always found good agreement when the experimental data were fitted with ΔE close to the L_{III} edge value (± 1 eV) and we can definitively exclude the single threshold model. In order to avoid a large number of free parameters, we fixed ΔE to the value obtained from the analysis of the L_{III} data (see Table I). The other input parameters in the simulations are n_f and the average Sm–first-neighbor distance $d_a=(d_{n+1}-d_n)/2$. With the preceding remarks in mind we checked that atomic relaxation variations larger than 0.02 Å can be evidenced from the data simulations presented in Sec. IV C.

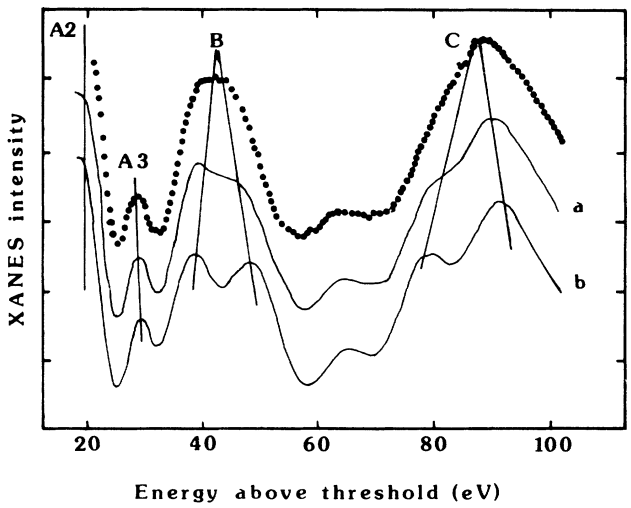

FIG. 3. Same as Fig. 2 with $\Delta E=7.5$ eV and different values of the atomic relaxation ΔR. (a) $\Delta R=0.04$ Å; (b) $\Delta R=0.1$ Å.

C. Data analysis

Here we present the XANES results above the Sm L_{III} edges of Fig. 1 for SmS and SmB_6 alloys. First, notice that we are dealing with structures at low energy above the edge, where contributions from light atoms are most important.[32,44] This remark has two kinds of outcomes: (i) The interatomic distance that enters in the $(E-E_0)d^2$ rule for rescaling the energy axis of the reference spectra can be identified with the first-neighbor distance (that is proportional to the lattice spacing in the NaCl or CaB_6 structure of these alloys). (ii) The substitution on the Sm site by other RE elements has only a weak influence on the one-electron contribution to the spectra. This contribution can therefore be safely approximated rescaling the energy axis of the reference spectra in order to take into account the variations of interatomic distances. This might not be true in the case of substitution on the anion site of SmS, so that we limited our analysis to the weakest doping contents producing the collapse into the metallic phase (10% P or 15% As).

XANES spectra for SmS (SmB_6) systems normalized after a smooth background substraction extending $\simeq 100$ eV above the Sm^{2+} threshold (used as the energy zero) are presented in Fig. 4 (Fig. 5) with decreasing $4f$ occupancy n_f. In both systems, a multiple-scattering resonance is observed around 30–40 eV. As n_f decreases, this resonance broadens (a clear splitting is even observed for $Sm_{0.96}As_{0.04}$) and shifts at higher energy ($\simeq 10$ eV). Taking into account the remarks of the Sec. II, this can be qualitatively understood by (i) the shift ($\simeq 7$ eV) of Sm^{3+} threshold with respect to Sm^{2+} (ii) the smaller size of Sm^{3+} ions that also moves the resonance at higher energy according to the scaling law as $(E-E_0)d^2$.

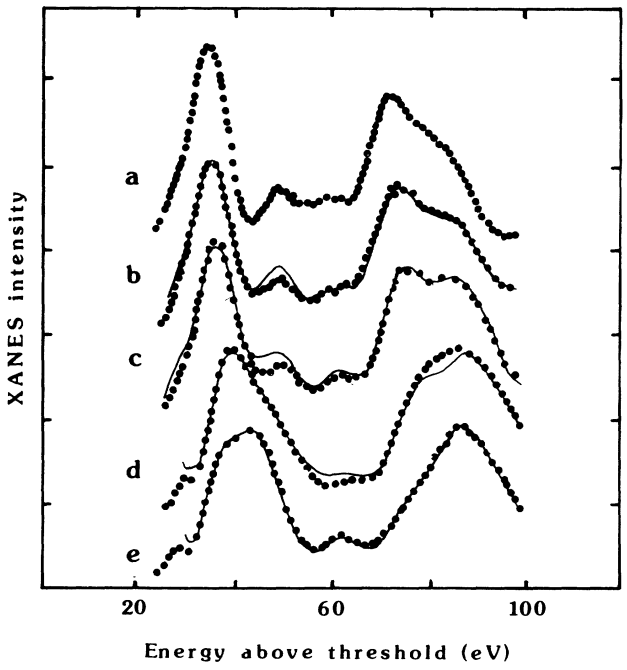

FIG. 4. Experimental L_{III} XANES (dots) and simulations with the parameters of Table I (full line) for the following samples: (a) SmS; (b) $Sm_{0.86}Gd_{0.14}S$; (c) $Sm_{0.75}Y_{0.25}S$ at 70 K; (d) $Sm_{0.75}Y_{0.25}S$; and (e) $Sm_{0.75}Gd_{0.25}S$. A graduation in the vertical scale represents 4% of the edge jump.

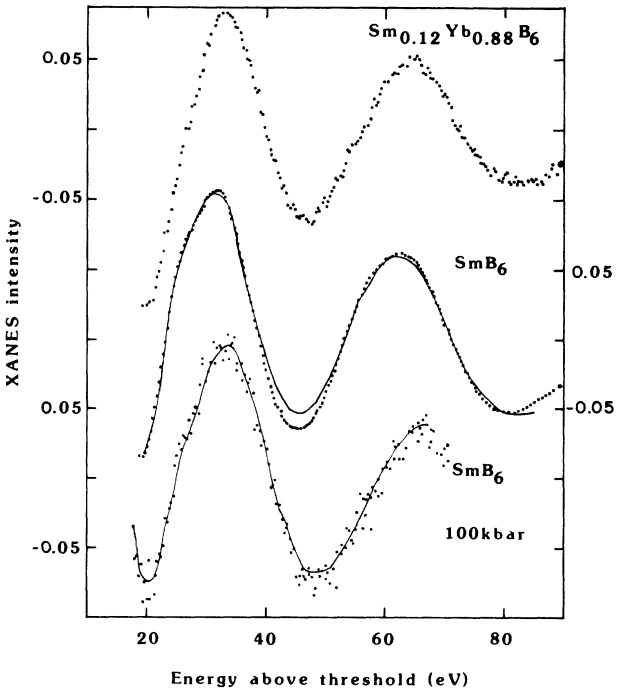

FIG. 5. Same as Fig. 4 for $Sm_{0.12}Yb_{0.88}B_6$ and SmB_6 at $P=0$ and 100 kbar. A graduation in the vertical scale represents 5% of the edge jump.

In order to obtain more quantitative information, we will now present simulations of the data using the method explained in the previous section. To do this, we used the experimental spectrum of SmS for which $a=5.97$ Å and $n_f=1$ ($Sm_{0.12}Yb_{0.88}B_6$; $a=4.14$ Å, $n_f=0.08\simeq 0$) as a reference for describing SmS (SmB_6) substitutional alloys. Such fits, with the parameters of Table I, are reported in Figs. 4 and 5 together with the experiments. The average first-neighbors interatomic distance deduced from our analysis, d_a, appears to be in good agreement (usually ± 0.01 Å, see Table I) with the lattice constant data. Considering the large variations in the shape of experimental spectra, this is a good *a posteriori* check of the validity of our analysis. It is particularly interesting to consider here the experiments performed under high pressure on SmB_6 (Fig. 5), since chemical disorder is here obviously absent and the modification of the Sm valence is only related to the shortening of the lattice constant. The reduced volume $V(P)/V(P=0)$ deduced from our XANES experiments tracks the values obtained by x-ray diffraction under pressure (Fig. 6). The distance determination from XANES spectra is not very accurate (± 0.03 Å) due to the poor statistics and the smaller extansion in energy of the spectra. However, we underline that such experiments bring additional information on x-ray diffraction due to the local nature of the x-ray-absorption process and concerning atomic relaxation effects.

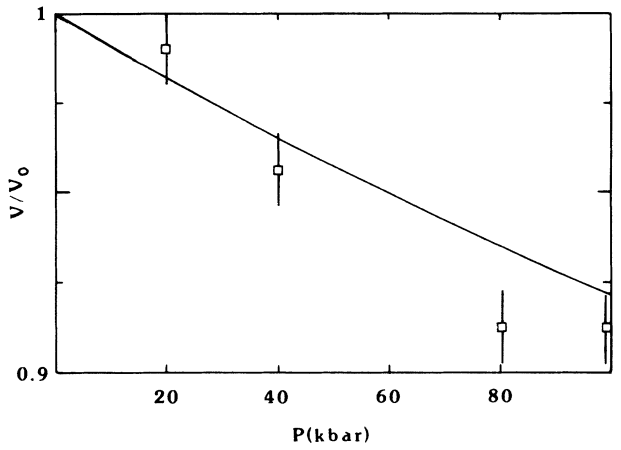

FIG. 6. Reduced volume $V(P)/V(P=0)$ of SmB_6 deduced from XANES experiments. Full line: x-ray-diffraction data of Ref. 47.

D. Discussion

Here we discuss the results of our XANES analysis (see Table I) in connection with the physical properties of the systems and the mechanism of x-ray-absorption spectroscopy.

The possibility for determining atomic relaxation effects from XANES data is one of the most important points of this study. The inspection of Table I shows that SmS samples in the pretransitional phase [i.e., $SmS_{0.96}As_{0.04}$ (Ref. 20)] and $Sm_{0.86}Gd_{0.14}S$) are characterized by large atomic relaxation ($\simeq 0.12$ Å) and are comparable to the difference between $Sm^{+2}S$ and $Sm^{+3}S$ distances (0.16 Å). This is in agreement with the IMV ground state of such samples.

By contrast, HMV systems (metallic SmS samples and SmB_6) can be classified as follows: Sm(S,As,P) and (Sm,Sr)B_6 alloys where atomic relaxations are vanishingly small within our accuracy (± 0.02 Å). This situation should be the result of the weak electron-phonon coupling limit,[43] where the interatomic distance adopts a single value. For anion site substituted (Sm,Y,Gd)S, ΔR is small but nonzero (0.03–0.05 Å at room temperature) as it has been observed for TmSe by EXAFS spectroscopy.[16] This is typical of the strong electron-phonon coupling limit: The electron phonon interactions are larger than the hybridization energy so that anomalies appear in the phonon spectra of these systems[6,7] due to the shell breathing. The comparison of our ΔR with calculations including phonon properties of SmS (Ref. 45) indicates a hybridization parameter $\Delta/\Pi \simeq 10$ meV, which is 1 order of magnitude smaller than the estimates for Ce (Ref. 3) or Yb (Ref. 5) MV systems.

The low-temperature semiconducting phase (the so-called B phase) of $Sm_xGd_{1-x}S$ samples with $x=0.18$ and 0.25 should be considered separately, since ΔR values ($\simeq 0.08$ Å) are found halfway between those of typical HMV and IMV systems. This suggests that during the time of an x-ray-absorption process mainly a static admixture of Sm atoms with different valence states is probed for these compounds that may be due to local inhomogeneities.

The situation of SmB_6 is also particularly attractive since a weak gap is observed at low temperature ($T<170$ K) that is attributed either to the Wigner crystallization of the conduction electrons[46] or to an f-d hybridization gap.[47] It is remarkable that applying a pressure around 50 kbar closes this gap[48] and corresponds to an inflection point in the variations of valence as a function of pressure.[24,49] We therefore analyze SmB_6 spectra in order to get atomic relaxations at low temperature ($T\simeq 40$ K), or high pressure ($P\simeq 100$ kbar). In each case we found $\Delta R=0$. This confirms that the existence of such a gap is not related to a transition HMV→IMV. We argue here that the results of our analysis on SmB_6 are quite different from those recently obtained by EXAFS above the Se K edge in the compound SmSe whose properties are similar.[50] In fact, it has been suggested that the closing of the gap by pressure effects in this latter system is accompanied by strong atomic relaxation effects ($\Delta R\simeq 0.1$ Å), which could result from the apparition of an IMV phase.

Finally, let us comment the values of the energy splitting ΔE between the energy threshold associated with Sm^{2+} and Sm^{3+} configurations that we used in our simulations (see Table I). These values have been extracted from the deconvolution of L_{III} data; we therefore assumed that these energy thresholds are independent of the photoelectron kinetic energy: They are identified with the onset of the transitions $2p\rightarrow 5\epsilon d$. However, RE $5d$ orbitals are somewhat localized around the atomic site and final-state electronic relaxation cannot be excluded *a priori* as we shall discuss later. This effect has been invoked in the case of Ce systems in order to explain quantitatively the difference between core-level spectroscopies (where three lines are observed due to the presence of $4f^2$ orbitals for final-state screening), and L_{III} or M_{III} absorption (only two lines are observed in MV systems).[19] We have tested two types of final-state interactions proposed in Ref. 19: Coulomb interaction between the $5d$ states and (i) the core hole (U_{dc}) or (ii) the $4f$ orbitals (U_{fd}). The effect of U_{dc} is to shift the white line (involving the unoccupied $5d$ orbitals) by roughly this quantity below the onset of transitions toward continuum states (this onset corresponds in principle to the energy position of the L_{III} x-ray photoemission peak). For instance, due to the localization of $3d$ orbitals in the first transition-metal series, this phenomenon has been indicated in the L_{III} edge of NiO.[51] We checked the influence of reasonable values of U_{dc} (up to a few eV) by shifting together both Sm^{2+} and Sm^{3+} thresholds to higher energy in our simulations, and found that our conclusions on atomic relaxation are not changed.

The existence of finite Coulomb repulsion U_{fd} between $4f$ electrons and $5d$ band states is a more difficult problem since the energy splitting ΔE deduced from the white line would then be smaller by U_{fd} (in a first-order approximation) than the value that should be applied to expanded states that are involved above about 15 eV after the edge. A systematic error on ΔE would then lead to errors on ΔR as demonstrated by the discussion of Sec.

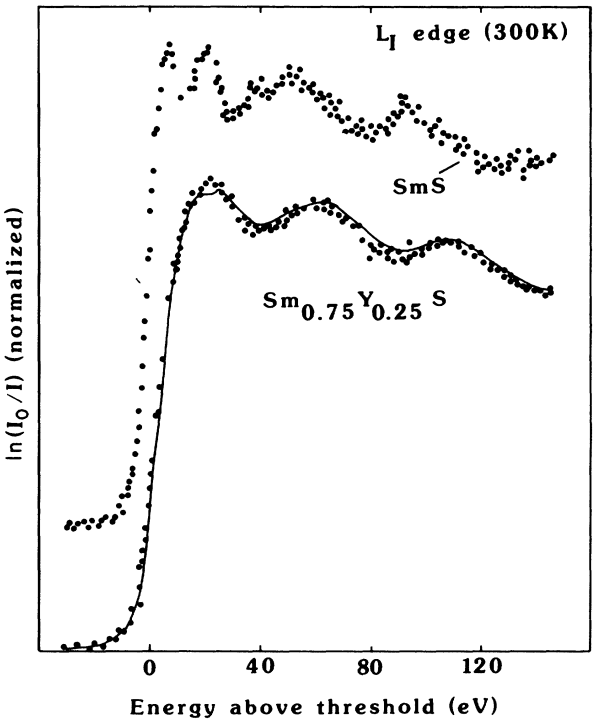

FIG. 7. Experimental L_I XANES recorded at 300 K (dots) and simulations (full line) as described in the text for SmS and $Sm_{0.75}Y_{0.25}S$.

II. On the other hand quantitative estimates of U_{fd} are not available for the moment and would require XPS experiments on L shells. Fruitful additional information can then be obtained from the comparison between L_{III} and L_I XANES (see also the discussion of Ref. 53); we report in Fig. 7 the L_I XANES of SmS and $Sm_{0.75}Y_{0.25}S$ recorded at room temperature. The dipole allowed transitions here are $2s^2 \rightarrow 2s^1 6\epsilon p$, involving much more extended states than in L_{III} or L_{II} spectroscopies, there result two advantages, though the signal-to-noise ratio is not as good: (i) No white line is observed in this energy range so that Sm^{2+} configuration energy threshold can be precisely measured as the first inflection point in the SmS spectrum (this is the zero in energy of Fig. 7). (ii) The corresponding parameter U_{fp} (repulsion between $4f$ and extended np states) is surely smaller than U_{fd}.

We simulated the $Sm_{0.78}Y_{0.25}S$ L_I XANES spectrum with the SmS reference and the parameters of Table I, except ΔE, which was adjusted to 8 eV (a reasonable value, taking into account the different nature of the $2p$ and $2s$ core hole). The good agreement with experiments, as shown in Fig. 7, permits us to conclude, for the moment, that neglecting U_{fd} in the interpretation of L_{III} XANES does not lead to contradictions between available experimental results.

V. CONCLUSIONS

We have shown in this paper that XANES spectra in mixed-valent Sm systems can be successfully analyzed taking into account both many-body and one-electron effects. Informations on structural (interatomic distances) and electronic properties (Sm valence), as well as their variation with alloy concentration, temperature, and hydrostatic pressure can then be obtained from such an analysis of the data.

The results of our XANES study on SmS and SmB_6 alloys show that Sm valence and interatomic distances, deduced from the simulations of these data, agree with the values obtained from other methods (e.g., respectively, L_{III} edges and lattice constant data). Moreover, these experiments are convincingly sensitive to atomic relaxation effects ± 0.02 Å,[20] and allow for the first time a systematic determination of this parameter for a large number of systems. In agreement with our earlier study, we found that atomic relaxations are large—comparable to the difference of ionic radii Sm^{2+}-Sm^{3+}—for IMV systems and much weaker (<0.1 Å) for HMV systems.

Our interpretation assumes that the final state of the x-ray-absorption process is built up by two noninterfering channels, corresponding here to Sm^{2+} and Sm^{3+} channels (this is equivalent to the convolution principle discussed in Ref. 39). As shown throughout this paper, this is a reasonable approximation that leads to interesting results but a complete understanding of the final-state interaction in XANES spectroscopy is still missing and is desirable. From a theoretical point of view, an application of the recent multichannel multiple-scattering theory[54] to mixed-valent systems should bring some justification to our analysis. On the other hand, photoemission spectroscopy on RE $2p$ levels is now under progress.[55] We expect that these experiments will allow (i) the determination of the energy threshold E_0 that enters the rescaling of the energy axis as a function of interatomic distances; (ii) checking whether final-state effects in the XANES regime can be described according to the ideas developed for RE $3d$ photoemission[3,4] or additional interactions should be taken into account, as seems to be the case for the light-RE L_{III} white line.[18,19]

ACKNOWLEDGMENTS

Thanks are due to C. Godart and D. Malterre for collaboration in the work on rare-earth systems. J. P. Senateur and J. Etourneau are gratefully acknowledged for providing us with some of the samples. One of us (J.P.K.) wishes to thank J. Röhler for a fruitful collaboration that allowed high-pressure experiments.

[1]P. W. Anderson, Phys. Rev. **124**, 41 (1961).

[2]T. V. Ramakrishnan, in *Valence Fluctuations in Solids,* edited by L. M. Falikov, W. Hanke, and M. P. Maple (North-Holland, Amsterdam, 1983), p. 13; P. W. Anderson, *ibid.*, p. 451.

[3]O. Gunnarsson and K. Schonhammer, Phys. Rev. B **28**, 4315 (1983).

[4]E. Wuilloud, B. Delley, W. D. Schneider, and Y. Baer, Phys. Rev. Lett. **53**, 202 (1985); A. Kotani, H. Mizuta, T. Jo, and J. P. Parlebas, Solid State Commun. **53**, 805 (1985).

[5]L. Degiorgi, T. Greber, F. Hulliger, R. Monnier, L. Schlappbach, and B. T. Thole, Europhys. Lett. **4**, 755 (1987).
[6]H. A. Mook and F. Holtzberg, in *Valence Fluctuations in Solids* (Ref. 2), p. 113.
[7]H. A. Mook, D. B. McWhan, and F. Holzberg, Phys. Rev. B **25**, 4321 (1982).
[8]L. Pintschovius, E. Holland-Moritz, D. K. Wohlleben, S. Stahr, and J. Lierbertz, Solid State Commun. **34**, 953 (1980).
[9]O. Blaschlko, G. Krexner, L. Pintschovius, W. Assmus, and G. Ernst, Solid State Commun. **51**, 971 (1984).
[10]R. Mock, E. Zirngiebl, B. Hillebrands, G. Guntherodt, and F. Holtzberg, Phys. Rev. Lett. **57**, 1040 (1986).
[11](a) R. M. Martin, J. B. Boyce, J. W. Allen, and F. Holtzberg, Phys. Rev. Lett. **44**, 1275 (1980); (b) J. B. Boyce, R. M. Martin, and J. W. Allen, in *EXAFS and Near Edge Structures*, edited by A. Bianconi, L. Incoccia, and S. Stipcich (Springer-Verlag, Berlin, 1983), p. 187.
[12]H. Launois, M. Raviso, E. Holland-Moritz, R. Pott, and D. Wohlleben, Phys. Rev. Lett. **44**, 1271 (1980).
[13]G. Krill, J. P. Kappler, and J. Rohler, in *EXAFS and Near Edge Structures* [Ref. 11(b)], p. 190.
[14]K. R. Bauchpiess, W. Boksch, E. Holland-Moritz, H. Launois, R. Pott, and D. Wohlleben, in *Valence Fluctuations in Solids* (Ref. 2), p. 417.
[15]G. Krill, J. P. Kappler, M. F. Ravet, C. Godart, and J. P. Senateur, J. Magn. Magn. Mater. **47&48**, 190 (1985).
[16]N. Wetta, G. Krill, P. Haen, F. Lapierre, M. F. Ravet, C. Godart, and F. Holtzberg, J. Phys. (Paris) Colloq. **47**, C8-965 (1986).
[17]S. Raaen, M. L. denBoer, V. Murgai, and R. D. Parks, Phys. Rev. B **27**, 5139 (1983).
[18]A. Bianconi *et al.*, Physica B **158**, 389 (1989).
[19]A. Kotani, J. Phys. (Paris) Colloq. **48**, C9-869 (1987).
[20]E. Beaurepaire, D. Malterre, J. P. Kappler, and G. Krill, Europhys. Lett. **5**, 369 (1988).
[21]J. M. Tarascon, Y. Isikawa, B. Chevalier, J. Etourneau, P. Hagenmuller, and M. Kasaya, J. Phys. (Paris) **41**, 1135 (1980).
[22]D. Ravot, C. Godart, J. C. Achard, and P. Lagarde, in *Valence Fluctuations in Solids* (Ref. 2), p. 423.
[23]E. Beaurepaire, G. Krill, J. P. Kappler, and J. Rohler, Solid State Commun. **49**, 65 (1984).
[24]J. Rohler, K. Keulertz, J. P. Kappler, and G. Krill, Laboratoire pour l'Utilisation du Rayonnement Electromagnétique Rapport d'Activite LURE 1984-1985 (unpublished).
[25]G. Materlik, J. E. Muller, and J. W. Wilkins, Phys. Rev. Lett. **50**, 267 (1983).
[26]O. Pena, R. Tournier, J. P. Senateur, and R. Fruchart, J. Magn. Magn. Mater. **15**, 13 (1980).
[27]S. Von Molnar, T. Penney, and F. Holtzberg, J. Phys. (Paris) Colloq. **37**, C4-241 (1976).
[28]L. J. Tao and F. Holtzberg, Phys. Rev. B **11**, 3842 (1975).
[29]C. Godart, J. C. Achart, G. Krill, and M. F. Ravet, J. Less-Common Met. **94**, 177 (1983), and references therein.
[30]J. Rohler, J. Magn. Magn. Mater. **47&48**, 175 (1985).
[31]J. Rohler, G. Krill, J. P. Kappler, and M. F. Ravet, in *EXAFS and Near Edge Structures* [Ref. 11(b)], p. 213.
[32]C. Brouder *et al.*, Physica B **158**, 495 (1989).
[33]J. Rohler, in *Handbook on the Physics and Chemistry of the Rare-Earths*, edited by K. A. Gschneidner, L. Eyring, and S. Hufner (Elsevier, New York, 1987), Vol. 10.
[34]E. Beaurepaire, J. P. Kappler, and G. Krill, Solid State Commun. **57**, 145 (1986).
[35]J. E. Muller, O. Jepsen, and J. W. Wilkins, Solid State Commun. **42**, 365 (1982).
[36]M. Alouani, J. M. Koch, and A. Khan, Solid State Commun. **60**, 657 (1986).
[37]C. R. Natoli and M. Benfatto, J. Phys. (Paris) Colloq. **47**, C8-11 (1986).
[38]B. Lengeler, G. Materlik, and J. E. Muller, Phys. Rev. B **28**, 2276 (1983).
[39]Y. Hammoud, J. C. Parlebas, and F. Gautier, J. Phys. F **17**, 503 (1987).
[40]G. Krill, J. P. Senateur, and A. Amamou, J. Phys. F **10**, 1989 (1980).
[41]D. Norman, J. Phys. C **19**, 3273 (1986), and references therein.
[42]C. R. Natoli, in *EXAFS and Near Edge Structures* [Ref. 11(b)], p. 43.
[43]K. Schonhammer and O. Gunnarson, Phys. Rev. B **30**, 3141 (1984).
[44]P. Saintctavit *et al.*, Physica B **158**, 347 (1989).
[45]W. Kohn, T. K. Lee, and Y. R. Lin-Lin, Phys. Rev. B **25**, 3557 (1982).
[46]T. Kasuya, K. Takegahara, Y. Aoki, K. Hanzawa, M. Kasaya, S. Kunii, T. Futjita, N. Sato, H. Kimura, T. Komatsubara, T. Furuno, and J. Rossa-Mignot, in *Valence Fluctuations in Solids* (Ref. 2), p. 215.
[47]P. Wachter and G. Travaglini, J. Magn. Magn. Mater. **47&48**, 423 (1985).
[48]V. V. Moshchalkov, I. V. Berman, N. B. Brandt, S. N. Pashkevich, E. V. Bogdanov, E. S. Konovalova, and M. V. Semenov, J. Magn. Magn. Mater. **47&48**, 289 (1985).
[49]K. B. Garg, D. Norman, and R. P. Beeken, Phys. Status Solidi A **96**, 301 (1986).
[50]K. R. Bauchspiess *et al.*, Physica B **158**, 492 (1989).
[51]G. Van der Laan, J. Zaanen, G. A. Sawatzky, R. Karnatak, and J. M. Esteva, Phys. Rev. B **33**, 4253 (1986).
[52]H. E. King, S. J. La Placa, T. Penney, and Z. Fisk, in *Valence Fluctuations in Solids* (Ref. 2), p. 333.
[53]G. Krill, J. P. Kappler, E. Beaurepaire, N. Wetta, D. Malterre, and C. Godart, in *Theoretical and Experimental Aspects of Valence Fluctuating and Heavy Fermions*, edited by L. C. Gupta and S. K. Malik (Plenum, New York, 1987), p. 205.
[54]C. R. Natoli and R. Benfatto, in *Core Level Spectroscopy in Condensed Systems*, edited by J. Kanamori and A. Kotani (Springer-Verlag, Berlin, 1988).
[55]D. Malterre, C. Brouder, G. Krill, E. Beaurepaire, J. P. Kappler, B. Carriere, and D. Chandesris, in Proceedings of the 2nd European Conference on Progress in X-Ray Synchrotron Radiation Research, Roma, 1989, [Nuovo Cimento (to be published)].